Cumulative influence of summer sub-surface soil temperature on North America surface temperature in NCEP CFSv2

Ravi P. Shukla[1,*] and Bohua Huang[1, 2]

[1]Center for Ocean-Land-Atmosphere Studies
George Mason University, Fairfax, Virginia, USA

[2]Department of Atmospheric, Oceanic, and Earth Sciences, George Mason University,
Fairfax, Virginia, USA

Contents of this file: Figures S1 to S13

[*]Corresponding author:
Ravi P. Shukla, PhD
Center for Ocean-Land-Atmosphere Studies (COLA)
George Mason University
270 Research Hall, Mail Stop 6C5,
4400 University Drive, Fairfax, VA 22030 USA
E-mail: rshukla2@gmu.edu

Figures Caption:

Figure S1. The spatial distributions of climatological seasonal mean of March to May (MAM) of H850 in (a) CFSR, (b) CFSv2 simulation and (c) climatological H850 biases relative to CFSR over the North America region. The scale for the magnitude for climatology (bias; gpm) of H850 is shown below these panels. **(d)-(f)** as in (a)-(c) but for MAM 850hPa-winds (m/s). The scale for the magnitude for climatology (bias) of 850hPa-winds is shown at left (right) of these panels. Spatial distributions of climatological MAM rainfall (mm/day) in **(g)** CMAP, **(h)** CFSv2 simulation and **(i)** climatological rainfall biases relative to CMAP. The scale for the magnitude for climatology (bias) of rainfall is shown at left (right) of these panels.

Figure S2. The spatial distributions of climatological seasonal mean of July to September (JAS) of H850 in **(a)** CFSR, **(b)** CFSv2 simulation and **(c)** climatological H850 biases relative to CFSR over the North America. The scale for the magnitude for climatology (bias; gpm) of H850 is shown below these panels. **(d)-(f)** as in (a)-(c) but for JAS 850hPa-winds (m/s). The scale for the magnitude for climatology (bias) of 850hPa-winds is shown at left (right) of these panels. Spatial distributions of climatological JAS rainfall (mm/day) in **(g)** CMAP, **(h)** CFSv2 simulation and **(i)** climatological rainfall biases relative to CMAP. The scale for the magnitude for climatology (bias) of rainfall is shown at left (right) of these panels.

Figure S3. **(a)** Spatial distribution of seasonal mean July to September (JAS) climatological ERA-Interim surface sensible heat flux (SSHF; W/m^2) over the North America. The scale for the magnitude for climatology of SSHF is shown at left of this figure. **(b)** The spatial distribution of climatological biases relative to SSHF ERA-Interim in model simulation during JAS. The scale for the magnitude for climatological bias of SSHF is shown at right of this figure. **(c)** as in (a) but for ERA-Interim surface latent heat flux (SLHF; W/m^2). **(d)** as in (b) but for SLHF in model simulation.

Figure S4. Spatial distribution of the climatological observed CERES-EBAF SCF SCF [%] in **(a)** Oct, **(b)** Nov, **(c)** Dec, **(d)** FEB, **(e)** MAR, **(f)** APR, **(g)** May and **(h)** Jun over the North America continent. The scale for the magnitude of SCF in "%" is shown below these panels. **(i)-(p)** as in (a)-(h) but for GLDAS-2.0 SWE [kg/m^2]. The scale for the magnitude of SWE in "kg/m^2" is shown right of these panels (1^{st}). **(q)-(x)** as in (a)-(h) but for CERES-EBAF Surface Albedo (SA). The scale for the magnitude of bias for SA in "%" is shown at right of these panels (2^{nd}).

Figure S5. Spatial distributions of monthly SWE [kg/m^2] climatological biases relative to reanalysis (GLDAS-2.0) in CFSv2 simulation for **(a)** Oct, **(b)** Nov, **(c)** Dec, **(d)** Feb, **(e)** Mar, **(f)** Apr, **(g)** May and **(h)** Jun over the North America continent. Monthly SCF climatological biases relative to observation in FIR for **(i)** Feb, **(j)** Mar, **(k)** Apr, **(l)** May and **(m)** Jun. Monthly SCF climatological biases relative to observation in MIR for (n) May and (o) June.

Figure S6. Spatial distributions of monthly Surface Albedo climatological biases relative to CERES-EBAF Surface Albedo (SA) in CFSv2 simulation for **(a)** Oct, **(b)** Nov, **(c)** Dec, **(d)** Feb, **(e)** Mar, **(f)** Apr, **(g)** May and **(h)** Jun. Monthly SA climatological biases relative to observation in FIR for **(i)** Feb, **(j)** Mar, **(k)** Apr, **(l)** May and **(m)** Jun. Monthly SA climatological biases relative to CERES-EBAF SA in MIR for **(n)** May and **(o)** June.

Figure S7. Spatial distribution of the climatological NOAA OISST v2 [^oC] in **(a)** SEP, **(b)** OCT, **(c)** NOV, **(d)** DEC, **(e)** FEB, **(f)** MAR, **(g)** APR and **(h)** MAY over the Northern Atlantic Ocean. The

red lines in all the panels depict 0 ºC (freezing temperature) in NOAA OISST v2. **(i)-(p)** as in (a)-(h) but for model simulation. (q)-(t) as in (e)-(h) but for FIR. The black line in all the panels depicts freezing temperature in simulation and reforecasts.

Figure S8. Spatial distribution of monthly climatological CFSR SUBT at 0-10cm [ºK] in **(a)** Jul, **(b)** Aug and **(c)** Sep. The scale for the magnitude for SUBT in ºK is shown at right of these panels. Both red and black lines in all the panels depict 273.15 ºK for CFSR (red line) and CFSv2 (black line). **(d)-(f)** as in (a)-(c) but for SUBT at 10-40cm. **(g)-(i)** as in (a)-(c) but for SUBT at 40-100cm. **(j)-(l)** as in (a)-(c) but for SUBT at 100-200cm.

Figure S9. Spatial distributions of monthly climatological LST biases relative to CFSR in CFSv2 simulation over the North America continent for **(a)** Apr, **(b)** May and **(c)** Jun. Both red and black lines in all the panels depict 273.15 ºK (freezing temperature) for CFSR (red line) and CFSv2 simulation (black line). **(d)-(e)** as in (a)-(c) but for SUBT at 0-10cm. **(d)-(e)** as in (a)-(c) but for SUBT at 10-40cm. **(d)-(e)** as in (a)-(c) but for SUBT at 40-100cm. **(d)-(e)** as in (a)-(c) but for SUBT at 100-200cm.

Figure S10. Difference between mean of five cold years and warm years of SUBT at 100-200cm over the America (outlined by green box in Figure 9; 44ºN-58ºN, 275ºE-298ºE) during July to September mean (JAS) in the CFSv2 simulation. **(b)** as in (a) SUBT at 0-10cm during October. The red line (black line) denotes 273.15ºK in cold year (warm year) in CFSv2. **(c)** as in (a) but for LST during October. **(d)** as in (a) but for SCF during October. **(e)-(h)** as in (a)-(d) but for CFSR reanalysis respectively.

Figure S11. **(a-e)** Spatial distribution of climatological bias for difference between subsurface SUBT at 100-200cm and SUBT 0-10cm relative to CFSR in FIR. **(f-i)** as in (a-e) but for MIR.

Figure S12. (**a-f**) Spatial distributions of monthly surface sensible heat flux (SSHF; W/m^2) climatological biases relative to reanalysis in model simulation during May to October over North America. **(g-l)** as in (a-f) but for net long wave radiation (LWR; W/m^2). The net LWR is defined as difference between downward LWR and upward LWR. **(m-r)** as in (a-f) but for net short wave radiation (SWR; W/m^2). The net SWR is defined as difference between downward SWR and upward SWR.

Figure S13: (a-f) Spatial distributions of monthly LST climatological biases (February to July) of the NCEP CFSv2 February initialized reforecast (FIR; 1982-2009) relative to CRU 3.21 (1979-2008) over the North America continent, monthly means based on the daily average of 6-hourly instantaneous values (i.e., 00Z, 06Z, 12Z, and 18Z) in NCEP CFSv2 FIR. **(g-l)** Spatial distributions of monthly mean LST climatological biases of NCEP CFSv2 FIR relative to CFSR (1979-2008), monthly means based on the daily average of 6-hourly instantaneous values (i.e., 00Z, 06Z, 12Z, and 18Z) in both reforecasts and reanalysis. (**m-r**) Spatial distributions of monthly LST climatological biases of CFSv2 FIR (1979-2008) relative to CFSR, monthly means based on the *instantaneous* fields at 00Z in both the CFSv2 FIR reforecasts and reanalysis.

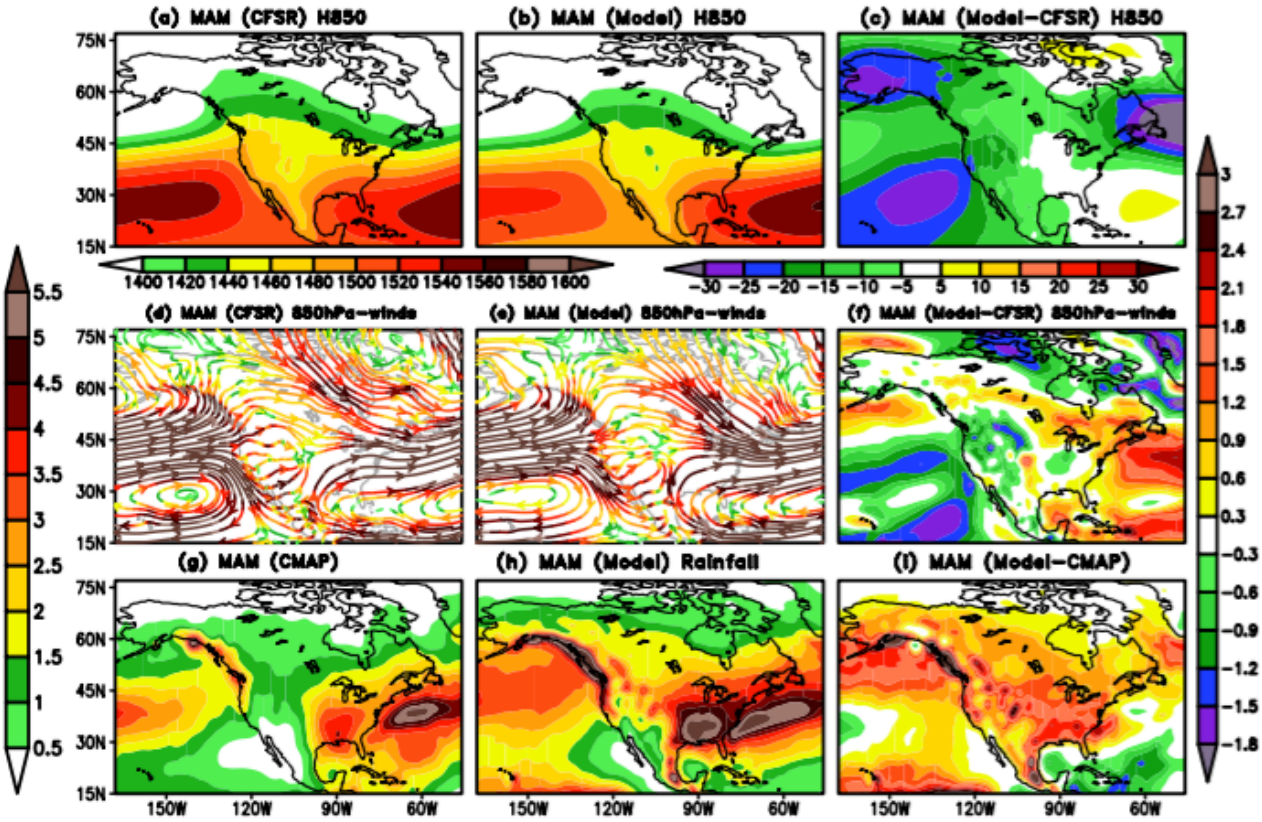

Figure S1. The spatial distributions of climatological seasonal mean of March to May (MAM) of H850 in (a) CFSR, (b) CFSv2 simulation and (c) climatological H850 biases relative to CFSR over the North America region. The scale for the magnitude for climatology (bias; gpm) of H850 is shown below these panels. **(d)-(f)** as in (a)-(c) but for MAM 850hPa-winds (m/s). The scale for the magnitude for climatology (bias) of 850hPa-winds is shown at left (right) of these panels. Spatial distributions of climatological MAM rainfall (mm/day) in **(g)** CMAP, **(h)** CFSv2 simulation and **(i)** climatological rainfall biases relative to CMAP. The scale for the magnitude for climatology (bias) of rainfall is shown at left (right) of these panels.

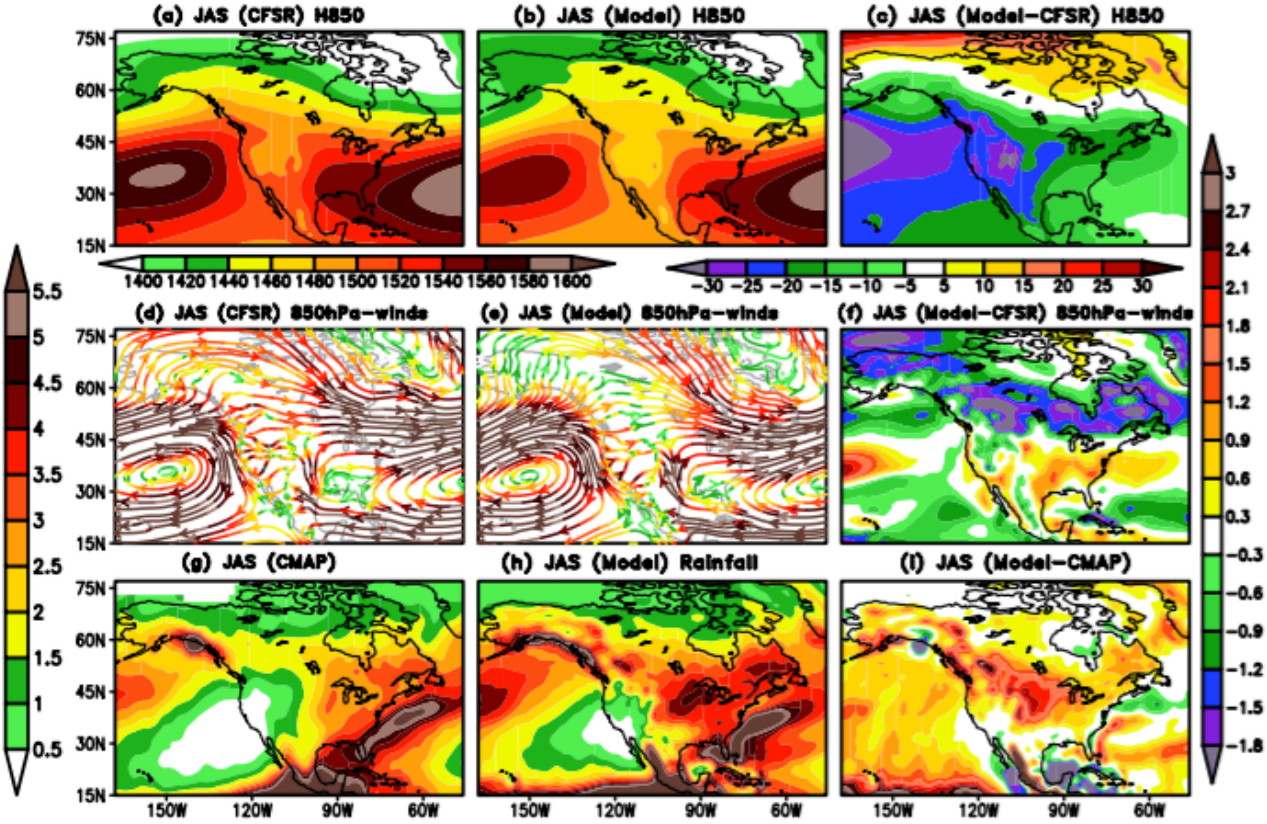

Figure S2. The spatial distributions of climatological seasonal mean of July to September (JAS) of H850 in **(a)** CFSR, **(b)** CFSv2 simulation and **(c)** climatological H850 biases relative to CFSR over the North America. The scale for the magnitude for climatology (bias; gpm) of H850 is shown below these panels. **(d)-(f)** as in (a)-(c) but for JAS 850hPa-winds (m/s). The scale for the magnitude for climatology (bias) of 850hPa-winds is shown at left (right) of these panels. Spatial distributions of climatological JAS rainfall (mm/day) in **(g)** CMAP, **(h)** CFSv2 simulation and **(i)** climatological rainfall biases relative to CMAP. The scale for the magnitude for climatology (bias) of rainfall is shown at left (right) of these panels.

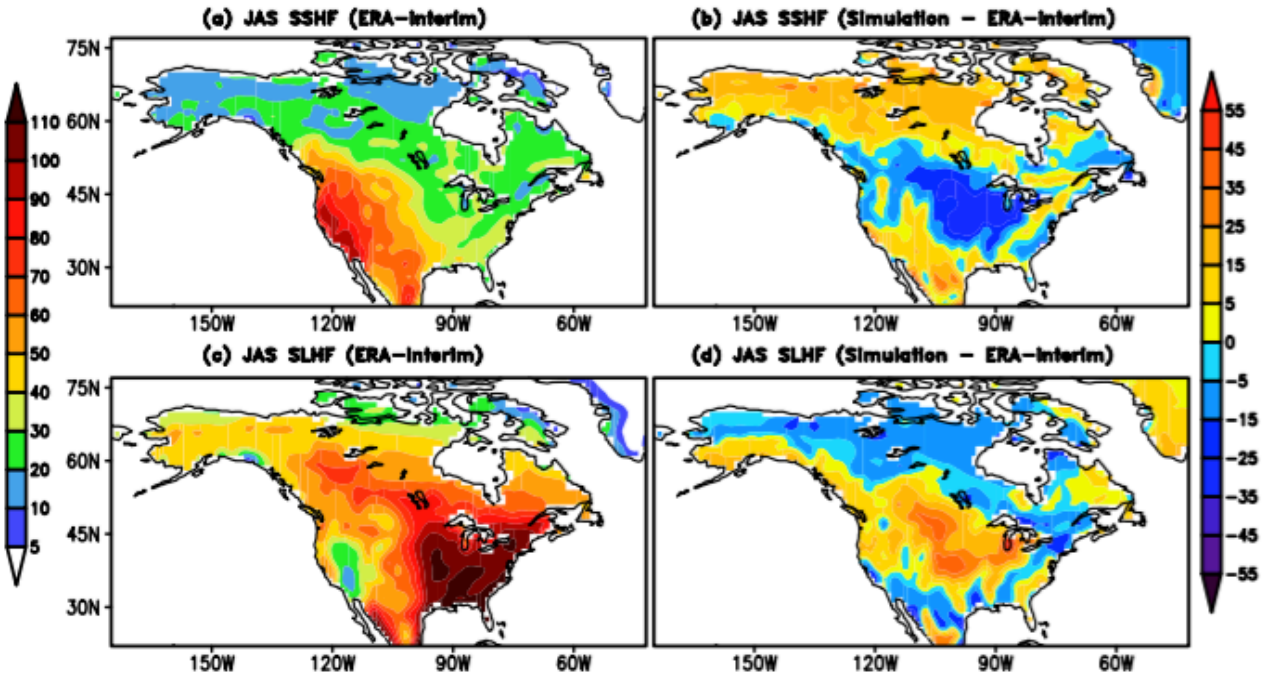

Figure S3. **(a)** Spatial distribution of seasonal mean July to September (JAS) climatological ERA-Interim surface sensible heat flux (SSHF; W/m^2) over the North America. The scale for the magnitude for climatology of SSHF is shown at left of this figure. **(b)** The spatial distribution of climatological biases relative to SSHF ERA-Interim in model simulation during JAS. The scale for the magnitude for climatological bias of SSHF is shown at right of this figure. **(c)** as in (a) but for ERA-Interim surface latent heat flux (SLHF; W/m^2). **(d)** as in (b) but for SLHF in model simulation.

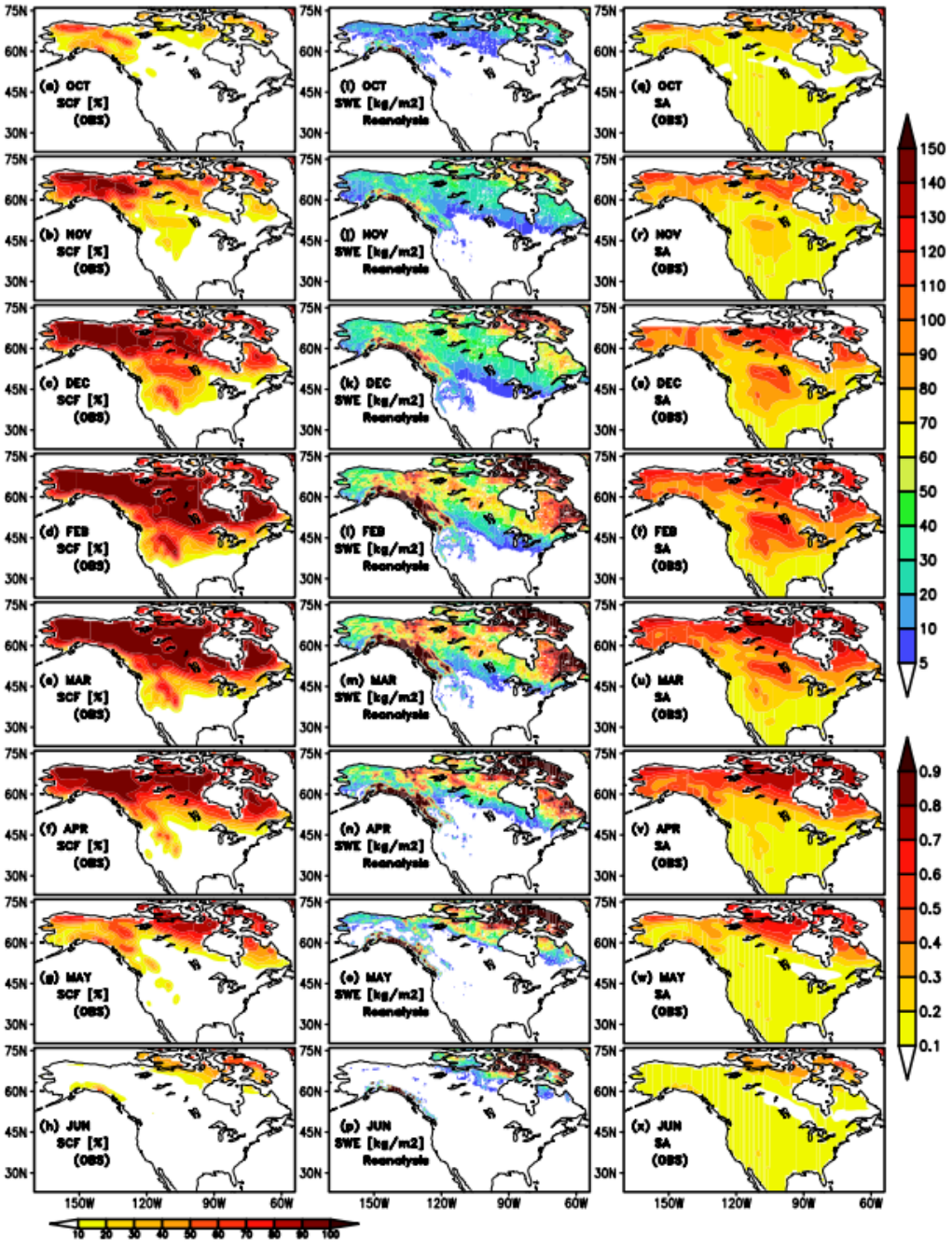

Figure S4. Spatial distribution of the climatological observed CERES-EBAF SCF SCF [%] in **(a)** Oct, **(b)** Nov, **(c)** Dec, **(d)** FEB, **(e)** MAR, **(f)** APR, **(g)** May and **(h)** Jun over the North America continent. The scale for the magnitude of SCF in "%" is shown below these panels. **(i)-(p)** as in (a)-(h) but for GLDAS-2.0 SWE [kg/m^2]. The scale for the magnitude of SWE in "kg/m^2" is shown right of these panels (1st). **(q)-(x)** as in (a)-(h) but for CERES-EBAF Surface Albedo (SA). The scale for the magnitude of bias for SA in "%" is shown at right of these panels (2nd).

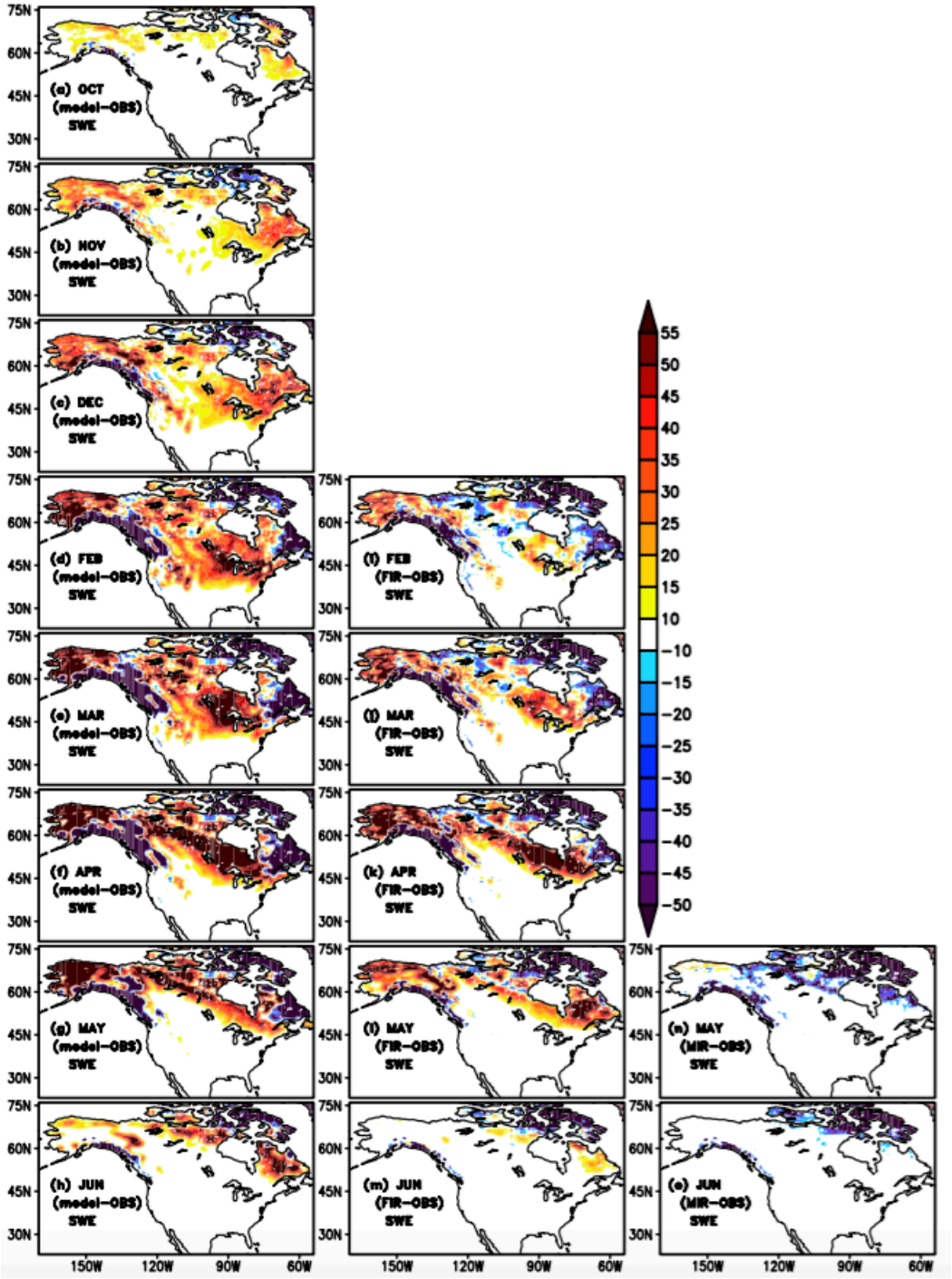

Figure S5. Spatial distributions of monthly SWE [kg/m^2] climatological biases relative to reanalysis (GLDAS-2.0) in CFSv2 simulation for **(a)** Oct, **(b)** Nov, **(c)** Dec, **(d)** Feb, **(e)** Mar, **(f)** Apr, **(g)** May and **(h)** Jun over the North America continent. Monthly SCF climatological biases relative to observation in FIR for **(i)** Feb, **(j)** Mar, **(k)** Apr, **(l)** May and **(m)** Jun. Monthly SCF climatological biases relative to observation in MIR for (n) May and (o) June.

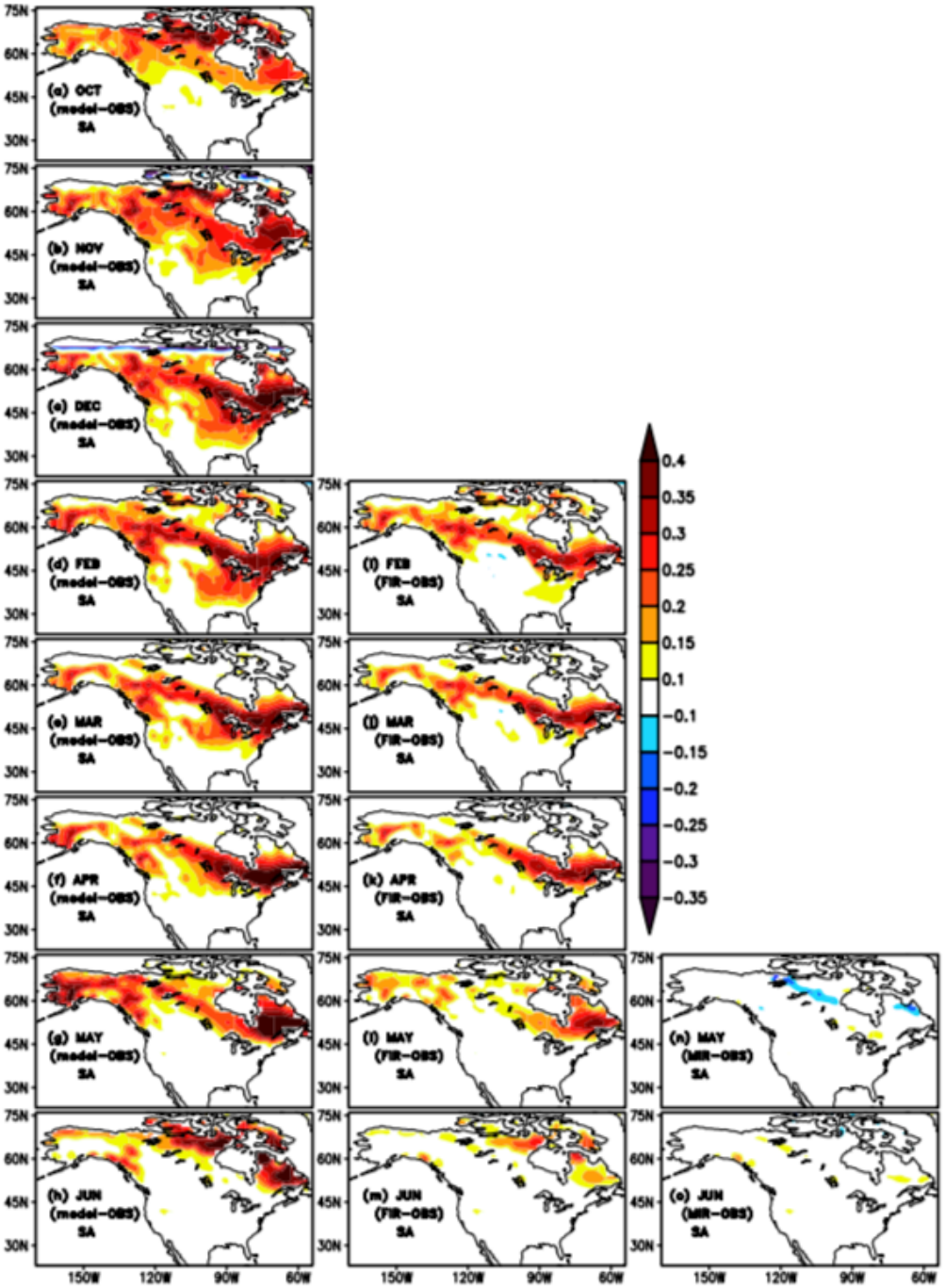

Figure S6. Spatial distributions of monthly Surface Albedo climatological biases relative to CERES-EBAF Surface Albedo (SA) in CFSv2 simulation for **(a)** Oct, **(b)** Nov, **(c)** Dec, **(d)** Feb, **(e)** Mar, **(f)** Apr, **(g)** May and **(h)** Jun. Monthly SA climatological biases relative to observation in FIR for **(i)** Feb, **(j)** Mar, **(k)** Apr, **(l)** May and **(m)** Jun. Monthly SA climatological biases relative to CERES-EBAF SA in MIR for **(n)** May and **(o)** June.

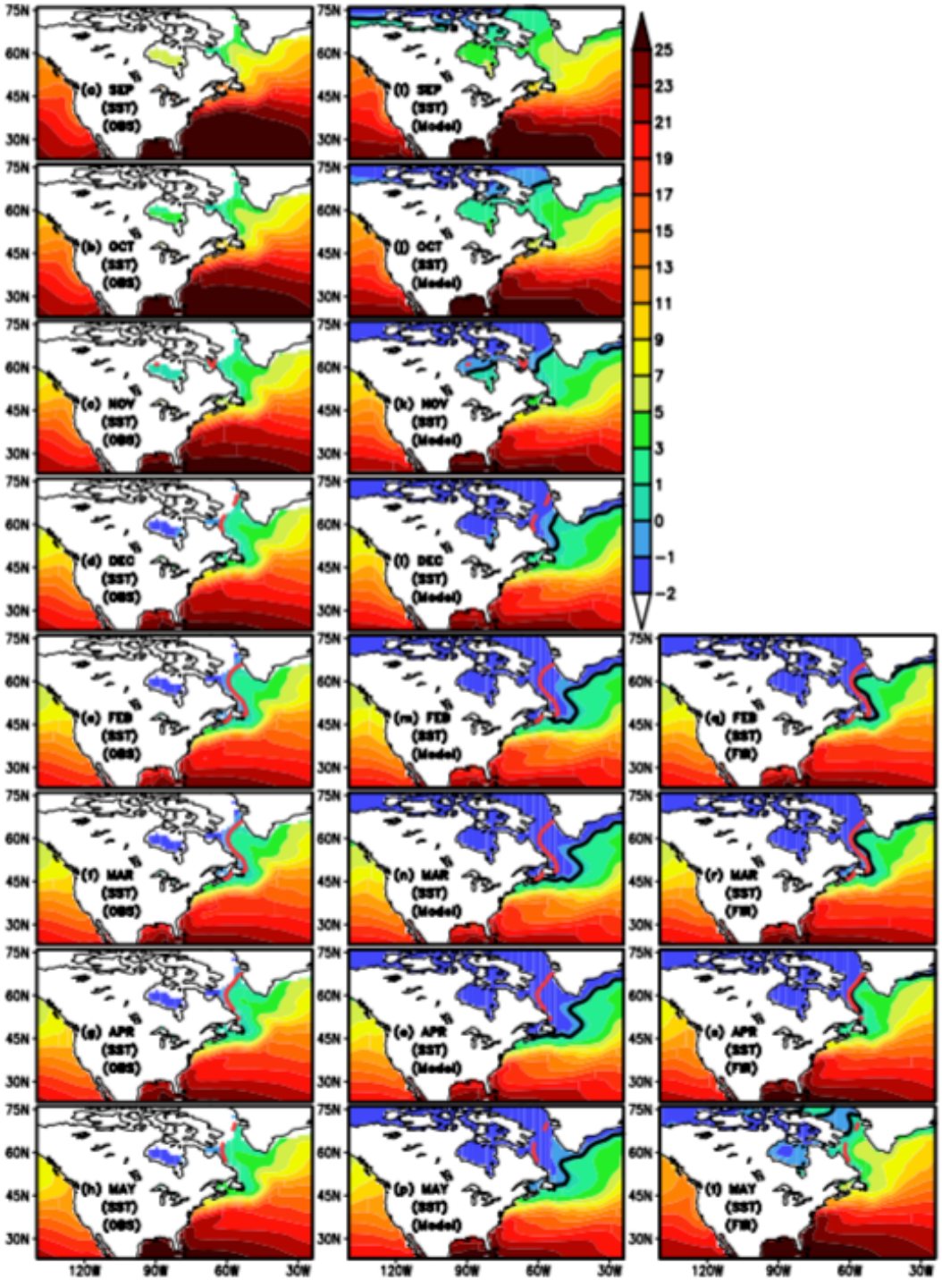

Figure S7. Spatial distribution of the climatological NOAA OISST v2 [ºC] in **(a)** SEP, **(b)** OCT, **(c)** NOV, **(d)** DEC, **(e)** FEB, **(f)** MAR, **(g)** APR and **(h)** MAY over the Northern Atlantic Ocean. The red lines in all the panels depict 0 ºC (freezing temperature) in NOAA OISST v2. **(i)-(p)** as in (a)-(h) but for model simulation. (q)-(t) as in (e)-(h) but for FIR. The black line in all the panels depicts freezing temperature in simulation and reforecasts.

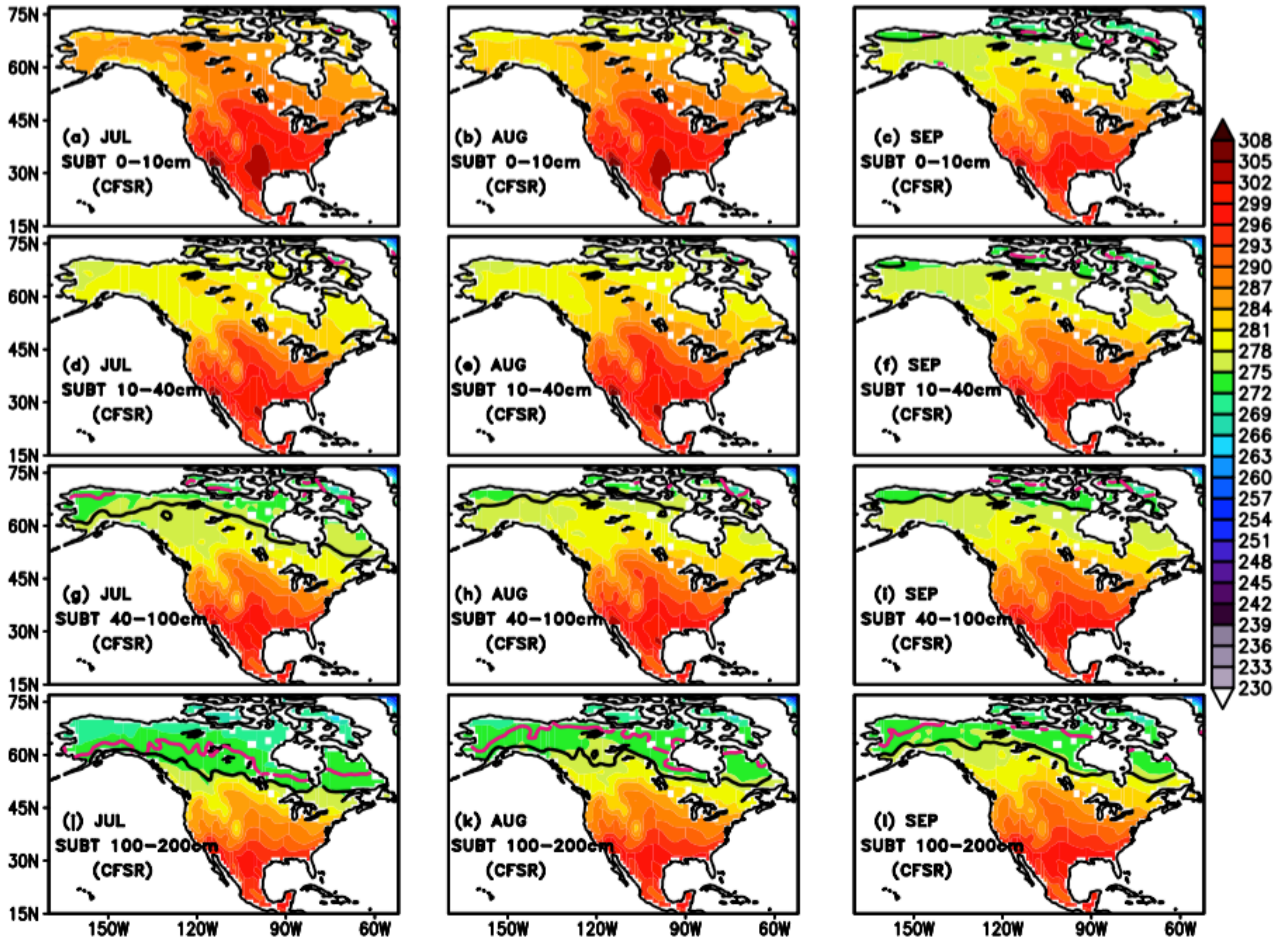

Figure S8. Spatial distribution of monthly climatological CFSR SUBT at 0-10cm [°K] in **(a)** Jul, **(b)** Aug and **(c)** Sep. The scale for the magnitude for SUBT in °K is shown at right of these panels. Both red and black lines in all the panels depict 273.15 °K for CFSR (red line) and CFSv2 (black line). **(d)-(f)** as in (a)-(c) but for SUBT at 10-40cm. **(g)-(i)** as in (a)-(c) but for SUBT at 40-100cm. **(j)-(l)** as in (a)-(c) but for SUBT at 100-200cm.

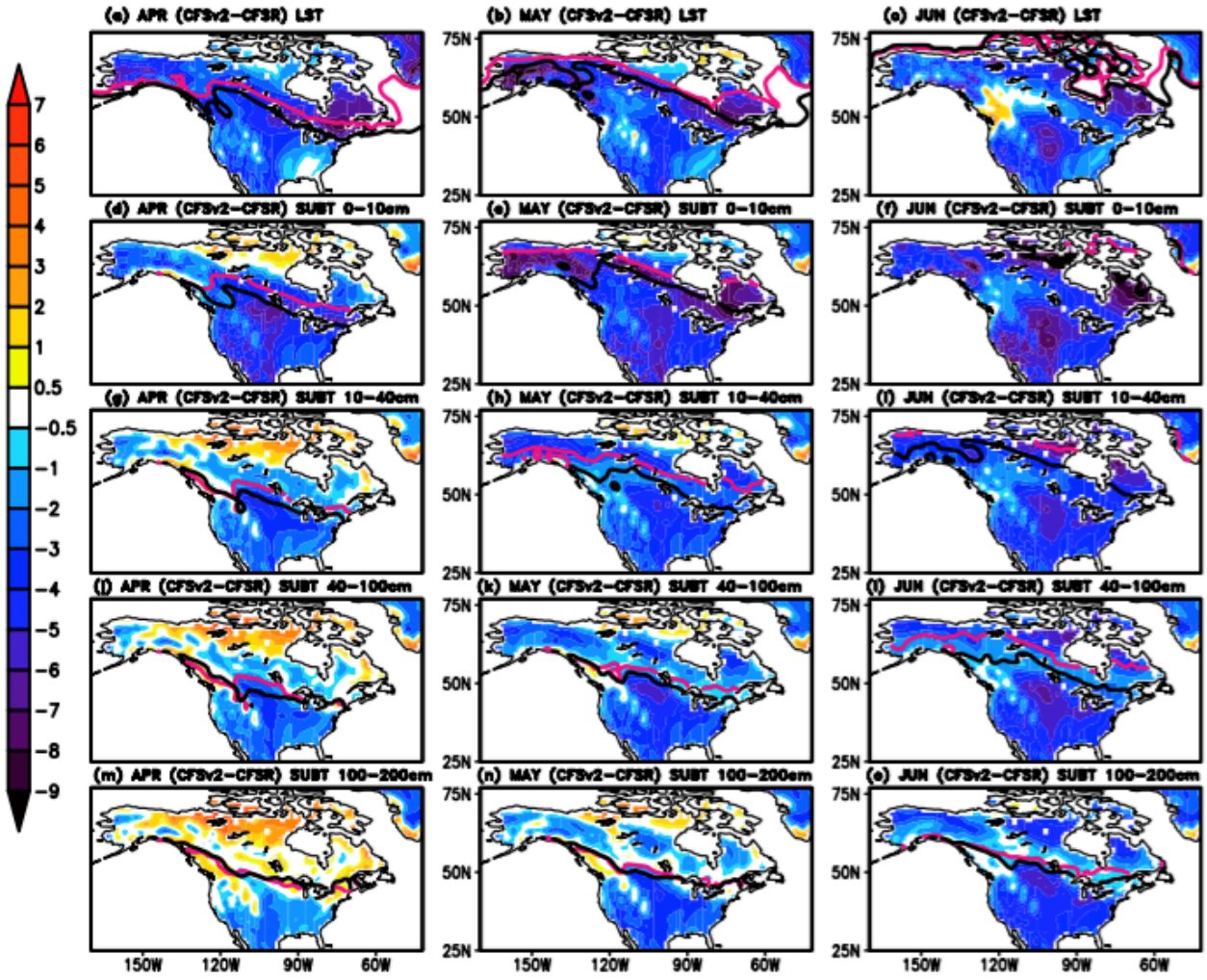

Figure S9. Spatial distributions of monthly climatological LST biases relative to CFSR in CFSv2 simulation over the North America continent for **(a)** Apr, **(b)** May and **(c)** Jun. Both red and black lines in all the panels depict 273.15 ^{o}K (freezing temperature) for CFSR (red line) and CFSv2 simulation (black line). **(d)-(e)** as in (a)-(c) but for SUBT at 0-10cm. **(d)-(e)** as in (a)-(c) but for SUBT at 10-40cm. **(d)-(e)** as in (a)-(c) but for SUBT at 40-100cm. **(d)-(e)** as in (a)-(c) but for SUBT at 100-200cm.

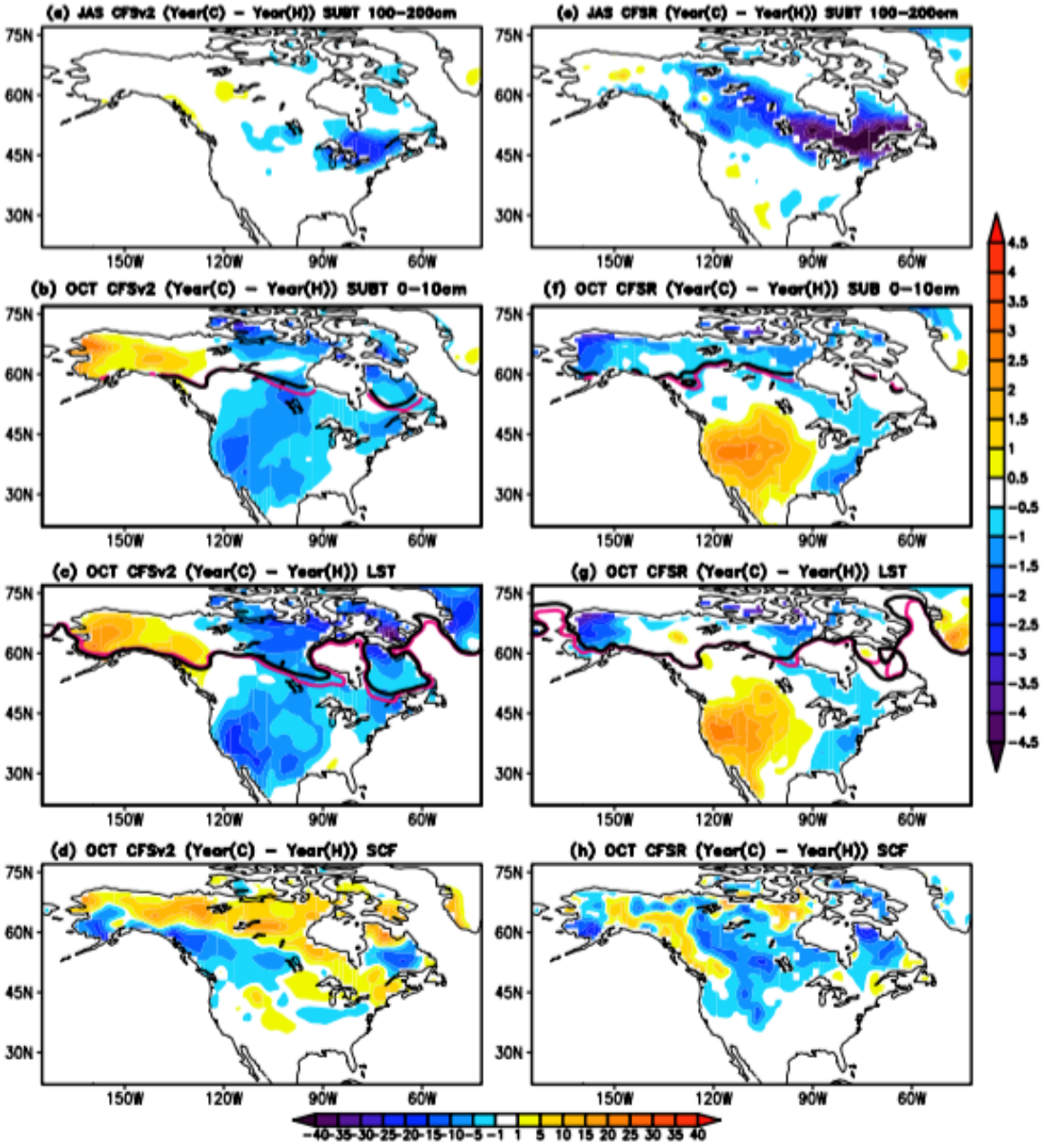

Figure S10. Difference between mean of five cold years and warm years of SUBT at 100-200cm over the America (outlined by green box in Figure 9; 44ºN-58ºN, 275ºE-298ºE) during July to September mean (JAS) in the CFSv2 simulation. **(b)** as in (a) SUBT at 0-10cm during October. The red line (black line) denotes 273.15ºK in cold year (warm year) in CFSv2. **(c)** as in (a) but for LST during October. **(d)** as in (a) but for SCF during October. **(e)-(h)** as in (a)-(d) but for CFSR reanalysis respectively.

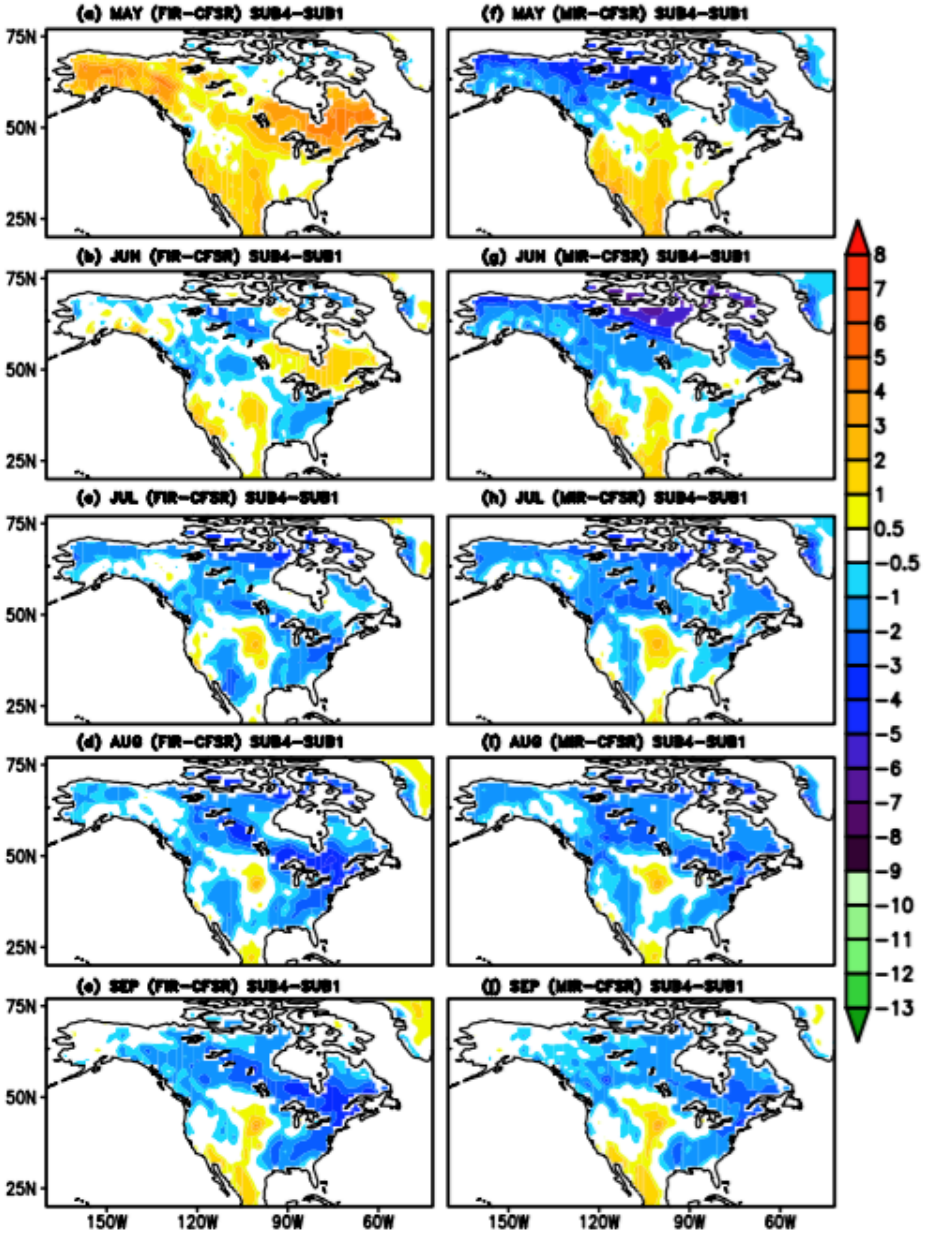

Figure S11. **(a-e)** Spatial distribution of climatological bias for difference between subsurface SUBT at 100-200cm and SUBT 0-10cm relative to CFSR in FIR. **(f-i)** as in (a-e) but for MIR.

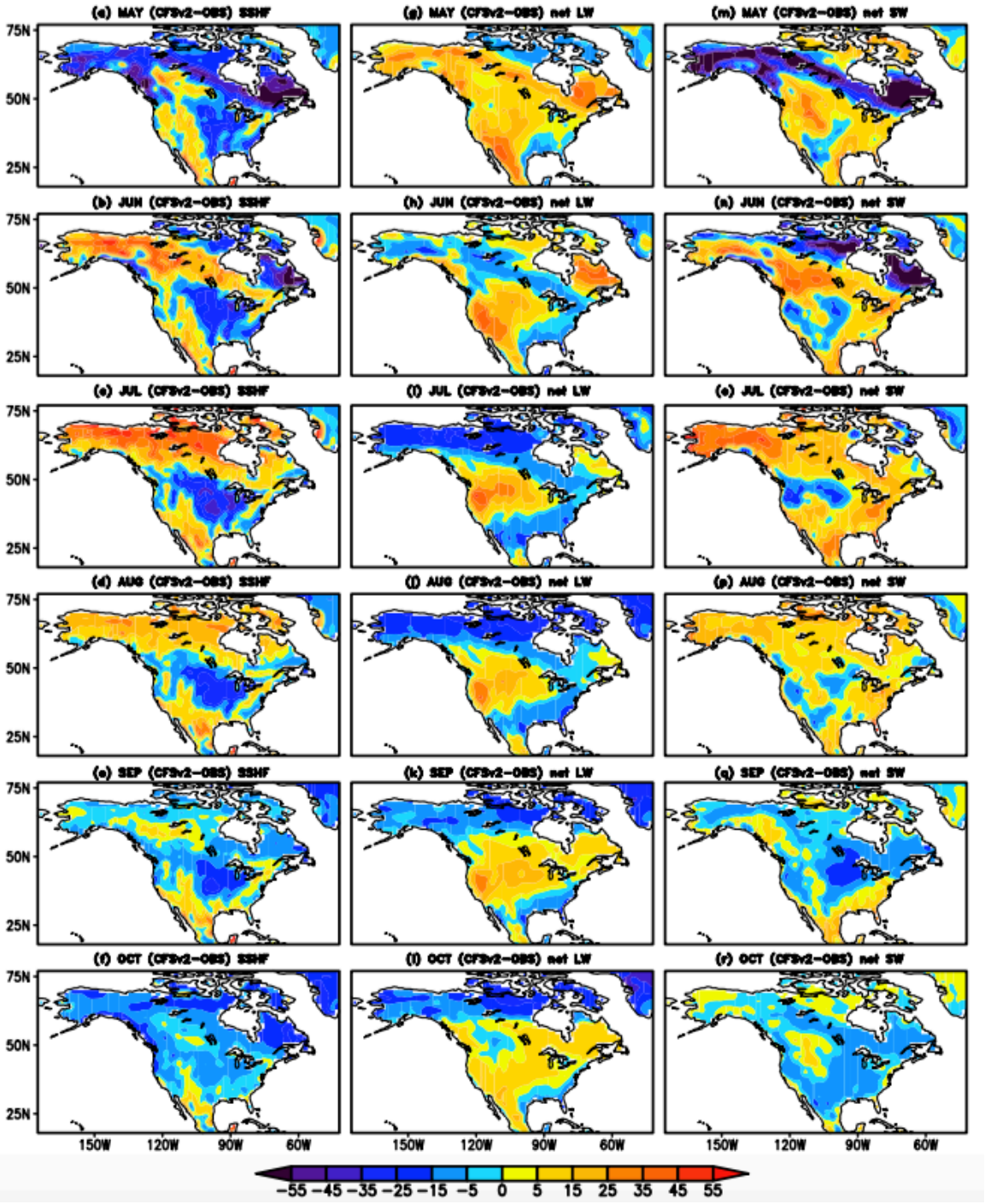

Figure S12. (**a-f**) Spatial distributions of monthly surface sensible heat flux (SSHF; W/m^2) climatological biases relative to reanalysis in model simulation during May to October over North America. (**g-l**) as in (a-f) but for net long wave radiation (LWR; W/m^2). The net LWR is defined as difference between downward LWR and upward LWR. (**m-r**) as in (a-f) but for net short wave radiation (SWR; W/m^2). The net SWR is defined as difference between downward SWR and upward SWR.

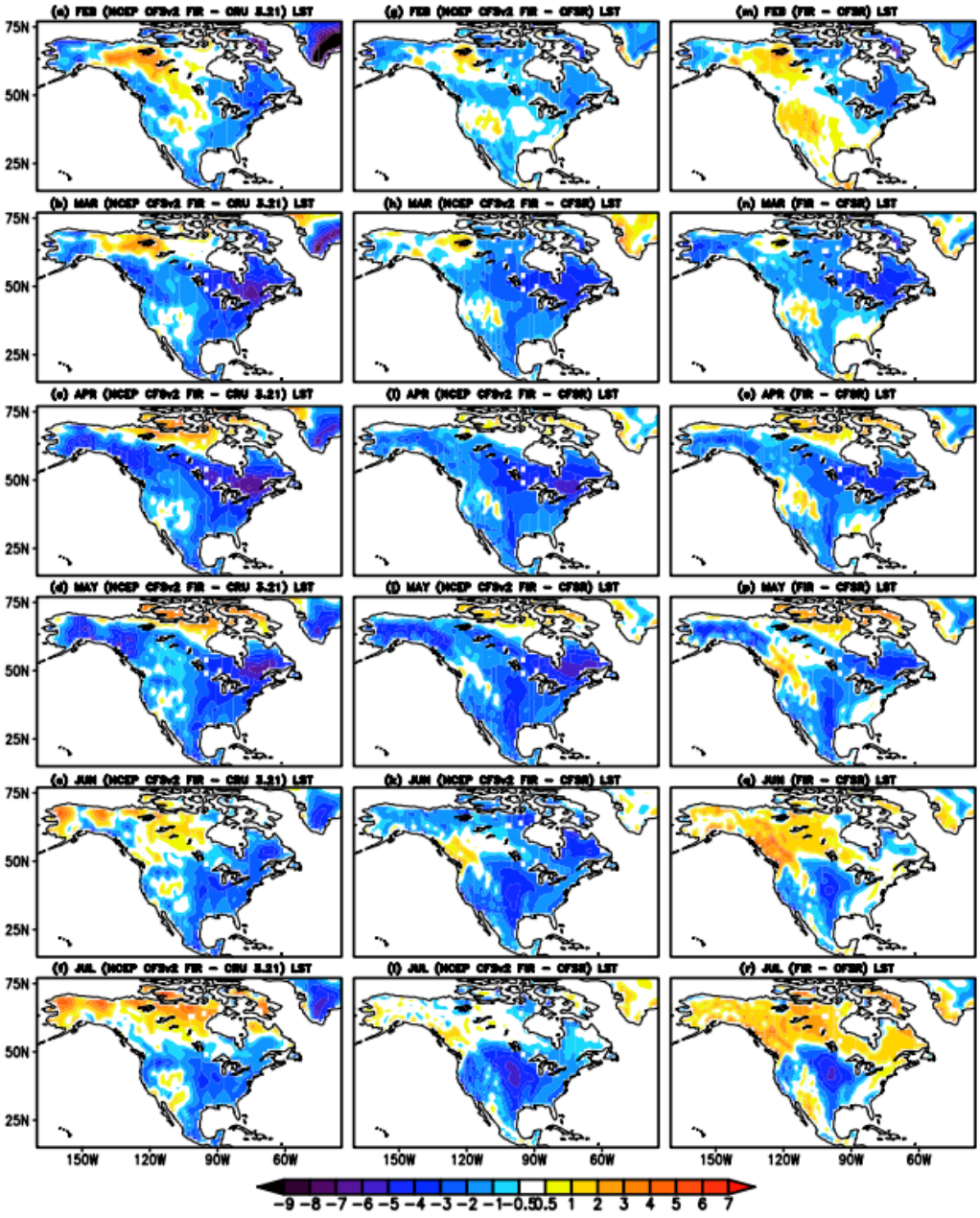

Figure S13: (a-f) Spatial distributions of monthly LST climatological biases (February to July) of the NCEP CFSv2 February initialized reforecast (FIR; 1982-2009) relative to CRU 3.21 (1979-2008) over the North America continent, monthly means based on the daily average of 6-hourly instantaneous values (i.e., 00Z, 06Z, 12Z, and 18Z) in NCEP CFSv2 FIR. **(g-l)** Spatial distributions of monthly mean LST climatological biases of NCEP CFSv2 FIR relative to CFSR (1979-2008), monthly means based on the daily average of 6-hourly instantaneous values (i.e., 00Z, 06Z, 12Z, and 18Z) in both reforecasts and reanalysis. **(m-r)** Spatial distributions of monthly LST climatological biases of CFSv2 FIR (1979-2008) relative to CFSR, monthly means based on the *instantaneous* fields at 00Z in both the CFSv2 FIR reforecasts and reanalysis.